Macromolecules

ARTICLE

pubs.acs.org/Macromolecules

2,7-Carbazole-1,4-phenylene Copolymers with Polar Side Chains for Cathode Modifications in Polymer Light-Emitting Diodes

Xiaofeng Xu, Bing Han, Junwu Chen,* Junbiao Peng, Hongbin Wu, and Yong Cao

Institute of Polymer Optoelectronic Materials & Devices, State Key Laboratory of Physics and Chemistry of Luminescence, South China University of Technology, Guangzhou 510640, China

ABSTRACT: Alcohol-soluble 2,7-carbazole-1,4-phenylene copolymers PCP-NOH and PCP-EP, comprising surfactant-like diethanolamino and phosphonate end groups on the side chains, respectively, were synthesized and utilized as electron injection layer (EIL) in combination with high work function Al electrode in polymer light-emitting diodes (PLEDs). The UV−vis absorption and photoluminescence properties of the PCP-NOH and PCP-EP are mainly determined by the conjugated 2,7-carbazole-1,4-phenylene main chain. The PCP-NOH and PCP-EP possess comparable HOMO levels of −5.20 eV and LUMO levels arround −2.35 eV. Multilayer PLEDs with a device configuration of ITO/PEDOT:PSS (40 nm)/emissive layer (70 nm)/EIL (15 nm)/Al (100 nm) were successfully fabricated. With fluorescent PFO-DBT15 as the emissive layer, the PLEDs using the PCP-NOH and PCP-EP as the EIL displayed luminous efficiency (LE) of 1.01 and 0.88 cd/A, respectively, all obviously higher than 0.015 cd/A for sole Al cathode and 0.58 cd/A for the well-known Ba/Al cathode. With a phosphorescent $Ir(mppy)_3$-doped polymer blend (PVK:PBD:$Ir(mppy)_3$ = 100:30:1) as the emissive layer, the PLEDs with the EIL showed high maximum LE of 39.3 cd/A for PCP-NOH and 42.5 cd/A for PCP-EP, in comparison to 0.35 cd/A for sole Al cathode and 32.2 cd/A for the Ba/Al cathode. Particularly, the PLED with PCP-EP as EIL exhibited an excellent LE of 33.3 cd/A at a current density of 61.1 mA/cm^2 (luminance = 20 300 cd/cm^2), showing weak roll-off of efficiency at high current density. Inserting the polar alcohol-soluble polymers as interlayer can significantly increase built-in potentials in the PLEDs, from which electron injection barrier from the Al electrode is decreased. The results indicate that the PCP-NOH and PCP-EP are excellent electron injection polymers for high-performance PLEDs with high work function Al electrode.

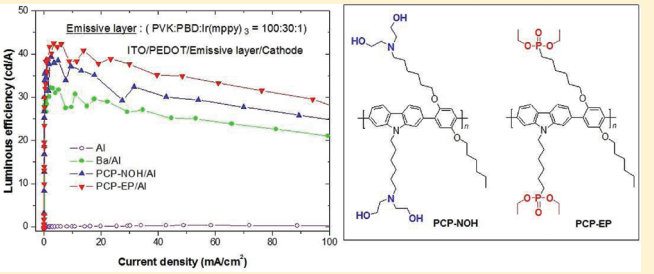

INTRODUCTION

During the past decade, polymer light-emitting diodes (PLEDs) have undergone significant improvements in efficiency, brightness, and drive voltage toward efficient full-color display panels and white-color illuminations.[1,2] PLEDs are carrier injection devices, whose balanced hole injection from the anode and electron injection from the cathode and their fast transports and recommbination in the emissive layer are the basic requirements.[3,4] Low work-function metals such as Ba and Ca are the widely utilized cathode materials to realize efficient electron injection. However, the low work-function metals are environmentally unstable, which can greatly affect the lifetime of PLEDs. Thus, it is desirable to use high work-function metals (Al, Ag, Au, etc.) as the cathode. Tremendous efforts have been paid to improve electron injection from high-work-function metals into the emissive layer. Inserting a thin layer of LiF, CsF, or some surfactants, between Al and the emissive layer, could significantly improve the electron injection.[5−8] However, all these methods showed cathode dependence, and they were not effective for other high-work-function metals such as Ag or Au. Recently, some alcohol/water-soluble polyfluorenes have been found excellent electron injection abilities in PLEDs.[9−11] It is the special solubility of the polyfluorenes in alcohol or water that makes sure the successful fabrications of PLEDs consisting multilayer polymers. Ammonium-functionalized cationic polyfluorenes and their neutral precursors are the early examples.[12−15] They could be utilized in PLEDs with Al or high work-function Ag or Au as the cathode.[16] For example, with PFN as a cathode interlayer, 80 and 200 times increases of luminous efficiency for Al and Ag, respectively, were reported for PLEDs with P-PPV as the emissive layer. A PLED with Au cathode almost did not emit detectable light; however, inserting PFN interlayer between P-PPV and Au could boost luminous efficiency to 11.6 cd/A. The PFN interlayer also established the feasibility of all-solution processed PLEDs with silver paste cathode to emit efficient red, green, and blue lights.[17] Using diethanolamino-functionalized polyfluorenes as cathode interlayer also exhibited excellent electron injection abilities, from which highly efficient PLEDs for green, blue, and white lights were demonstrated.[18−21] A phosphonate-functionalized polyfluorene as cathode interlayer for white PLEDs realized a forward viewing luminous efficiency of 15.4 cd/A.[22] A series of ammonium-functionalized cationic

Received: January 27, 2011
Revised: April 28, 2011
Published: May 10, 2011

polyfluorenes with different counteranions were synthesized to ellucidate their structure/function relationship.[23,24] It was proposed that dipole formation or ionic charge redistribution might contribute to the distinguished electron injection properties of the interlayer.[13,23] It should be pointed that using the alcohol/water-soluble polyfluorenes as interlayer in bulk-heterojunction photovoltaic cells[25−27] and n-channel thin-film transistors (TFTs)[28,29] also improved thier performances, demonstrating the important roles of the interlayer.

It is of interest for polymer chemists to develop new alcohol/water-soluble polymers. Polycarbazoles have an electron-rich main chain and a large band gap, known as typical p-type semiconductors.[30−35] Compared with the large family of fluorene-based alcohol/water-soluble conjugated polymers,[12,14,15,18,20−24,27] introducing a carbazole as a main chain building block to construct new interlayer polymers for optoelectronic devices receives much less attention. In this work, two new 2,7-carbazole-1, 4-phenylene copolymers PCP-NOH and PCP-EP, soluble in alcohol, were synthesized via transformation of a precursor polymer and one-step polymerization, respectively (Scheme 1). PCP-NOH and PCP-EP comprise surfactant-like diethanolamino and phosphonate end groups on the side chains of the both main chain blocks, respectively, which impart the alcohol solubilities of the two polymers. UV−vis absorption, photoluminescence (PL), and electrochemical property of the two polymers were characterized. Moreover, the two polymers were utilized to fabricate interlayer for electron injection from Al electrode in PLEDs with emissive layers based on a fluorescent polymer and a phosphorescent dye-doped polymer blend. With PFO-DBT15,[36] a typical fluoresecent polymer with saturated red-light emission, as the emissive layer, the PLEDs with PCP-NOH/Al and PCP-EP/Al bilayer cathodes displayed luminous efficiencies (LE) of 1.01 and 0.88 cd/A, respectively, all obviously higher than 0.015 cd/A for sole Al cathode and 0.58 cd/A for the well-known Ba/Al cathode. Iridium tris(2-(4-tolyl)pyridinato-$N,C^{2'}$) ($Ir(mppy)_3$),[37] a green-emitting phosphorescent dye, and 2-(4-biphenylyl)-5-(4-*tert*-butylphenyl)-1,3,4-oxadiazole (PBD), an electron transport material, were doped in poly (*N*-vinylcarbazole) (PVK) host with a blend ratio of PVK:PBD:$Ir(mppy)_3$ = 100:30:1. The phosphorescent PLEDs with PCP-NOH/Al and PCP-EP/Al bilayer cathodes showed maximum LE values of 39.3 and 42.5 cd/A, respectively, in comparison with 0.35 cd/A for sole Al cathode and 32.2 cd/A for the Ba/Al cathode. The results clearly demonstrate that PCP-NON and PCP-EP, synthesized in this work, can realize excellent electron injection in combination with high work function Al electrode for PLEDs with different emissive materials.

EXPERIMENTAL SECTION

Materials. All reagents and solvents, unless otherwise specified, were obtained from Aldrich, Acros, and TCI Chemical Co. and were used as received. Anhydrous tetrahydrofuran was distilled over sodium/benzophenone under N_2 prior to use. All manipulations involving air-sensitive reagents were performed under an atmosphere of dry argon. PVK and PBD were purchased from Aldrich, and $Ir(mppy)_3$ was from America Dye Source, Inc. All of them were used as received. Tetrabutylammonium hexafluorophosphate (Bu_4NPF_6) was recrystallized twice from a 50:50 mixture of methanol/water and dried at 60 °C under vacuum.

Instrumentations. ^1H and ^{13}C NMR spectra were recorded on a Bruker AV 300 spectrometer with tetramethylsilane (TMS) as the internal reference. Mass (MS) spectrometry was performed on an Esquire HCT PLUS operating in an atmospheric-pressure chemical ionization (APCI) mode. Melting points (mp) were obtained by a Gallenkamp melting point apparatus. Molecular weights of the polymers were obtained on a Waters GPC 2410 using a calibration curve of polystyrene standards, with tetrahydrofuran as the eluent. Elemental analyses were performed on a Vario EL elemental analysis instrument (Elementar Co.). UV−vis absorption spectra were recorded on a HP 8453 spectrophotometer. The PL spectra of the copolymer were obtained on a Jobin Yvon Fluorolog-3 spectrofluorometer. Cyclic voltammetry was carried out on a CHI660A electrochemical workstation with platinum electrodes at a scan rate of 50 mV/s against an Ag/Ag^+ reference electrode with a nitrogen-saturated solution of 0.1 M tetrabutylammonium hexafluorophosphate (Bu_4NPF_6) in acetonitrile (CH_3CN). The deposition of a copolymer on the electrode was done by the evaporation of a dilute THF solution.

2,7-Dibromo-9-(6′-bromohexyl)carbazole (1). 2,7-Dibromocarbazole (1.32 g, 4.1 mmol) in 10 mL of anhydrous THF was mixed with sodium hydride (0.20 g, 8.2 mmol) in 10 mL of anhydrous THF under an argon atmosphere. The reaction mixture was stirred at 60 °C for 1 h and then added to 1,6-dibromohexane (3.00 g, 12.3 mmol) in 50 mL of anhydrous THF. The reaction mixture was refluxed for 18 h. After cooling to room temperature, the solvent was removed under reduced pressure, and the oil phase was extracted with dichloromethane (100 mL), washed successively with water, and then dried over anhydrous $MgSO_4$. The residue was purified by column chromatography with 1:5 (v/v) dichloromethane/petroleum ether as the eluent to afford the title compound (1.40 g, 72%). White solid, mp: 104−105 °C. ^1H NMR (300 MHz, $CDCl_3$), δ (ppm): 7.88 (d, J = 8.3 Hz, 2H), 7.52 (s, 2H), 7.34 (d, J = 9.9 Hz, 2H), 4.20 (t, J = 7.2 Hz, 2H), 3.51 (t, J = 6.5 Hz, 2H), 1.84 (m, 2H), 1.78 (m, 2H), 1.51 (m, 2H), 1.45 (m, 2H). ^{13}C NMR (75 MHz, $CDCl_3$), δ (ppm): 141.3, 122.6, 121.5, 121.3, 119.7, 112.0, 44.8, 43.2, 32.4, 28.7, 26.6, 26.5. Anal. Calcd for $C_{18}H_{18}Br_3N$: C, 44.30; H, 3.72; N, 2.87. Found: C, 44.41; H, 3.83; N, 2.89. MS (APCI): 489.2 $[(M + 1)^+]$.

2,7-Bis(4,4,5,5-tetramethyl-1,3,2-dioxaborolan-2-yl)-*N*-(6-bromohexyl)carbazole (2). 2,7-Dibromo-9-(6′-bromohexyl) carbazole, **1** (1.40 g, 2.87 mmol), bis(pinacolato)diboron (2.19 g, 8.61 mmol), potassium acetate (2.53 g, 25.83 mmol), and $PdCl_2$(dppf) (0.07 g, 0.09 mmol) were dissolved in 50 mL of anhydrous dioxane. The reaction mixture was heated to 80 °C for 8 h under an argon atmosphere. After cooling to room temperature, the organic layer was extracted with dichloromethane (100 mL), washed successively with water, and then dried over anhydrous $MgSO_4$. The residue was purified by column chromatography with 1:2 (v/v) dichloromethane/petroleum ether as the eluent and recrystallized from THF/ethanol to give the final compound (1.39 g, 83%): white solid; mp: 203−204 °C. ^1H NMR (300 MHz, $CDCl_3$), δ (ppm): 8.13 (d, J = 7.8 Hz, 2H), 7.88 (s, 2H), 7.69 (d, J = 7.8 Hz, 2H), 4.41 (t, J = 7.1 Hz, 2H), 3.51 (t, J = 6.7 Hz, 2H), 1.92 (m, 2H), 1.73 (m, 2H), 1.56−1.41 (br, m, 28H). ^{13}C NMR ($CDCl_3$, 75 MHz), δ (ppm): 140.4, 125.1, 124.9, 120.0, 115.2, 83.8, 45.0, 42.6, 32.5, 29.1, 26.7, 26.4, 24.9. Anal. Calcd (%) for $C_{30}H_{42}B_2BrNO_4$: C, 61.89; H, 7.27; N, 2.41. Found: C, 62.19; H, 7.40; N, 2.43. MS (APCI): 583.2 $[(M + 1)^+]$.

Diethyl 6-(2,7-Bis(4,4,5,5-tetramethyl-1,3,2-dioxaborolan-2-yl)carbazol-9-yl)hexylphosphonate (3). A solution of 2,7-bis-(4,4,5,5-tetramethyl-1,3,2-dioxaborolan-2-yl)-*N*-(6-bromohexyl)carbazole, **2** (1.46 g, 2.5 mmol), in triethyl phosphate was heated to 140 °C under an argon atmosphere for 24 h. Then the excess triethyl phosphate was distilled in a vacuum, and the crude product was purified by silica chromatography (ethyl acetate/ether = 1:1) to give the title compound (1.52 g, 95%): white solid; mp: 94−95 °C. ^1H NMR ($CDCl_3$, 300 MHz), δ (ppm): 8.12 (d, J = 9.8 Hz, 2H), 7.86 (s, 2H), 7.68 (d, J = 9.7 Hz, 2H),

Scheme 1

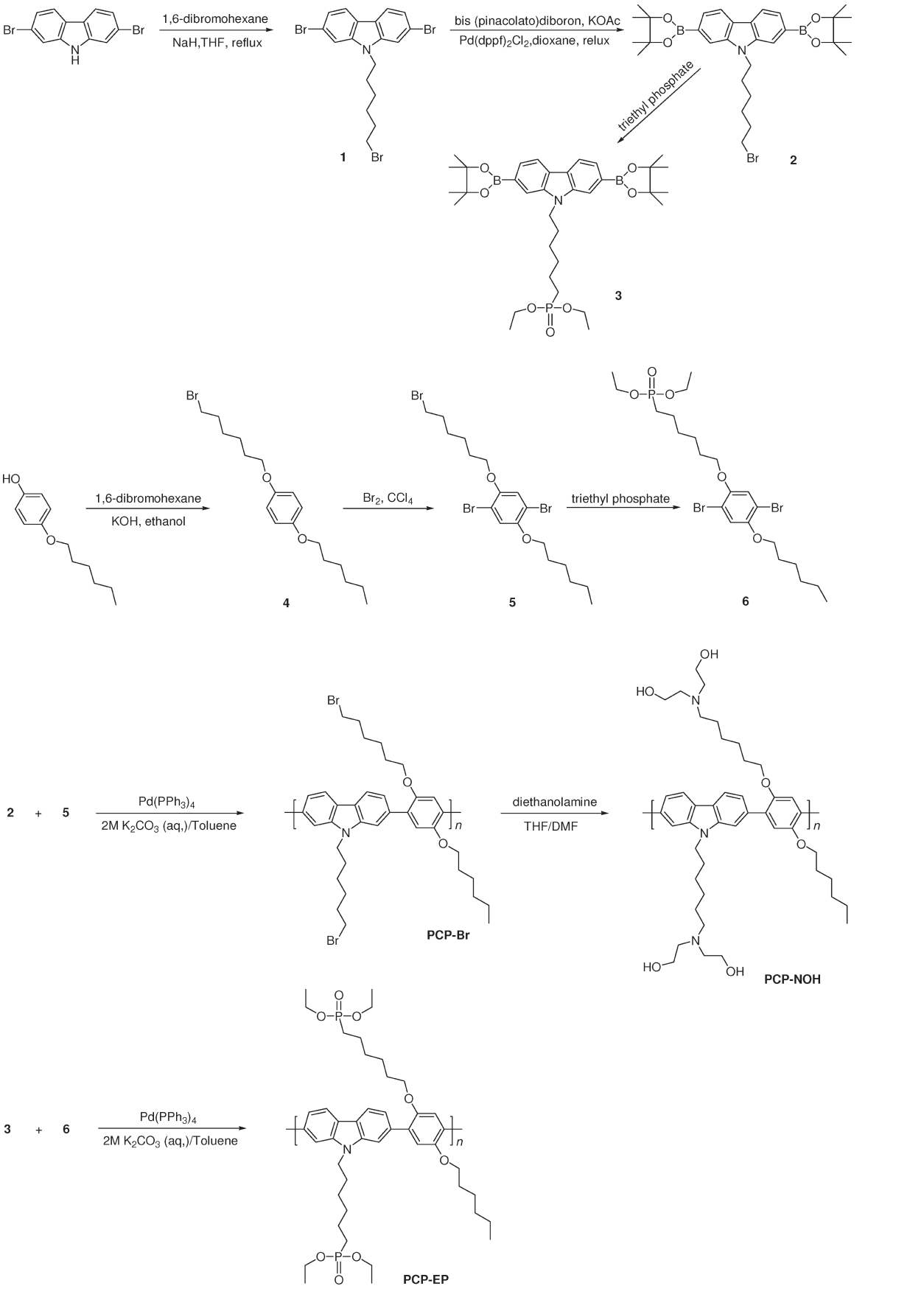

dx.doi.org/10.1021/ma200191p |*Macromolecules* 2011, 44, 4204–4212

4.38 (t, J = 6.3 Hz, 2H), 4.05 (m, 4H), 1.90 (m, 2H), 1.69 (m, 6H), 1.40 (br, s, 26H), 1.29 (t, J = 7.0 Hz, 6H). ^{13}C NMR ($CDCl_3$, 75 MHz), δ (ppm): 140.4, 125.1, 124.9, 120.0, 115.2, 83.8, 61.4, 42.8, 30.6, 30.4, 29.1, 26.7, 24.9, 22.4, 16.5. Anal. Calcd (%) for $C_{34}H_{52}B_2NO_7P$: C, 63.87; H, 8.20; N, 2.19. Found: C, 62.72; H, 8.46; N, 2.16. MS (APCI): 640.5 [$(M + 1)^+$].

1-(6-Bromohexyloxy)-4-hexyloxybenzene (4). Potassium hydroxide (0.67 g, 12.0 mmol) in 30 mL of methanol was mixed with 4-hexyloxyphenol (1.94 g, 10.0 mmol) in 30 mL of methanol under an argon atmosphere. The reaction mixture was stirred for 1 h and then added to 1,6-dibromohexane (7.32 g, 30.0 mmol) in 50 mL of acetone. The reaction mixture was refluxed for 12 h. After cooling to room temperature, the solvent was removed under reduced pressure. The organic phase was extracted with dichloromethane (100 mL), washed successively with water, and then dried over anhydrous $MgSO_4$. After removal of the solvent, the residue was purified by column chromatography (dichloromethane/petroleum ether = 1:4 as the eluent) to give the title compound (2.5 g, 70%): white solid, mp: 39−40 °C. ^{1}H NMR ($CDCl_3$, 300 MHz), δ (ppm): 6.81 (s, 4H), 3.89 (m, 4H), 3.42 (m, 2H), 1.89 (m, 2H), 1.75 (m, 4H), 1.51 (m, 6H), 1.34 (m, 4H), 0.90 (m, 3H). ^{13}C NMR ($CDCl_3$, 75 MHz), δ (ppm): 153.3, 153.1, 115.43, 115.41, 68.7, 68.4, 33.8, 32.7, 31.6, 29.4, 29.2, 28.0, 25.7, 25.3, 22.6, 14.0. Anal. Calcd (%) for $C_{18}H_{29}BrO_2$: C, 60.50; H, 8.18. Found: C, 60.62; H, 8.24. MS (APCI): 358.3 [$(M + 1)^+$].

1,4-Dibromo-2-(6-bromohexyloxy)-5-hexyloxybenzene (5). 1-(6-Bromohexyloxy)-4-hexyloxybenzene, **4** (2.49 g, 7.0 mmol), was dissolved in 100 mL of CCl_4 and stirred below 5 °C. Bromine (0.8 mL, 15.5 mmol) was added dropwise to the solution over 30 min. The resulting solution was stirred overnight. The remaining bromine was quenched by the addition of saturated aqueous $Na_2S_2O_3$ (100 mL), and then the organic layer was extracted with dichloromethane (100 mL). The organic phase was washed successively with water and then dried over anhydrous $MgSO_4$. After removal of the solvent, the residue was purified by column chromatography (dichloromethane/petroleum ether = 1:3 as the eluent) and recrystallized from ethanol to give the final compound (3.00 g, 83%): white solid; mp: 57−58 °C. ^{1}H NMR ($CDCl_3$, 300 MHz), δ (ppm): 7.08 (s, 2H), 3.94 (m, 4H), 3.42 (m, 2H), 1.90 (m, 2H), 1.80 (m, 4H), 1.52 (m, 6H), 1.35 (m, 4H), 0.91 (m, 3H). ^{13}C NMR ($CDCl_3$, 75 MHz), δ (ppm): 150.2, 150.0, 118.50, 111.2, 70.3, 70.1, 33.7, 32.7, 31.5, 29.1, 28.9, 27.8, 25.6, 25.2, 22.6, 14.0. Anal. Calcd (%) for $C_{18}H_{27}Br_3O_2$: C, 41.97; H, 5.28. Found: C, 42.09; H, 5.43. MS (APCI): 516.1 [$(M + 1)^+$].

1,4-Dibromo-2-(6-(diethylphosphoryl)hexyloxy)-5-hexyloxybenzene (6). A solution of 1,4-dibromo-2-(6-bromohexyloxy)-5-hexyloxybenzene, **5** (1.64 g, 3.0 mmol), in triethyl phosphate was heated to 140 °C under an argon atmosphere for 24 h. Then the excess triethyl phosphate was distilled in a vacuum, and the crude product was purified by silica chromatography (ethyl acetate/diethyl ether = 1:1 as the eluent) to give the title compound (1.60 g, 93%): white solid; mp: 48−49 °C. ^{1}H NMR ($CDCl_3$, 300 MHz), δ (ppm): 7.08 (s, 2H), 4.09 (m, 4H), 3.95 (m, 4H), 1.85−1.60 (m, 8H), 1.49 (m, 6H), 1.34 (m, 10H), 0.91 (m, 3H). ^{13}C NMR ($CDCl_3$, 75 MHz), δ (ppm): 150.2, 150.0, 118.5, 111.2, 70.3, 70.1, 61.4, 31.5, 30.3, 30.1, 29.0, 26.6, 25.5, 24.7, 22.6, 22.3, 16.5, 14.0. Anal. Calcd (%) for $C_{22}H_{37}Br_2O_5P$: C, 46.17; H, 6.52. Found: C, 46.11; H, 6.69. MS (APCI): 573.3 [$(M + 1)^+$].

Polymerization. Polymerizations of PCP-Br and PCP-EP were carried out by palladium(0)-catalyzed Suzuki coupling reactions with equivalently molar ratio of a diboronic ester monomer to a dibromo monomer under argon protection. The purifications of the polymers were conducted in air. The preparation of PCP-NOH was carried out by a transformation reaction based on PCP-Br.

Poly[(*N*-(6′-bromohexyl)-2,7-carbazole)-*alt*-(2-hexyloxy-5-(6′-bromohexyloxy)-1,4-phenylene)] (PCP-Br). 2,7-Bis(4,4,5,5-tetramethyl-1,3,2-dioxaborolan-2-yl)-*N*-(6-bromohexyl)carbazole (0.292 g, 0.5 mmol), 1,4-dibromo-2-(6-bromohexyloxy)-5-hexyloxybenzene (0.258 g, 0.5 mmol), $Pd(PPh_3)_4$ (12 mg), and 3 drops of Aliquat336 were dissolved in a mixture of 12 mL of toluene and 2 mL of 2 M K_2CO_3 aqueous solution. The mixture was refluxed with vigorous stirring for 1 day under an argon atmosphere. After the mixture was cooled to room temperature, it was poured into 250 mL of methanol. The precipitated material was redissolved and filtrated through a funnel and then precipitated again. The resulting solid material was washed successively with acetone for 24 h and dried in vacuum to afford the title polymer as a white solid (341 mg, 62%). GPC: M_n = 10.5 kDa; M_w/M_n = 2.3. ^{1}H NMR ($CDCl_3$, 300 MHz), δ (ppm): 8.19 (br, 2H), 7.75 (br, 2H), 7.53 (br, 2H), 7.24 (br, 2H), 4.41 (br, 2H), 4.03 (br, 4H), 3.39−3.29 (d, 4H), 2.00−1.28 (m, 24H), 0.85 (br, 3H). Anal. Calcd (%) for $(C_{36}H_{45}Br_2O_2N)_n$: C, 63.25; 6.59, N, 2.05. Found: C, 64.61; H, 6.33; N, 1.95.

Poly[(9-(*N*,*N*-di(2″-hydroxyethyl)-6′-aminohexyl)-2,7-carbazole)-*alt*-(2-hexyloxy-5-(*N*,*N*-di(2″-hydroxyethyl)-6′-aminohexyloxy)-1,4-phenylene)] (PCP-NOH). Diethanolamine (0.5 g) was added to a solution of PCP-Br (100 mg) in a mixture of 20 mL of THF and 5 mL of DMF. The mixture was stirred vigorously for 48 h at 60 °C under an argon atmosphere. After cooling to room temperature, the mixture was poured into 250 mL of H_2O. The resulting polymer was then collected and dried in vacuum to afford the final polymer as a white solid (89 mg, 82%). ^{1}H NMR ($CDCl_3$, 300 MHz), δ (ppm): 8.18 (br, 2H), 7.75 (br, 2H), 7.50 (br, 2H), 7.22 (br, 2H), 4.39 (br, 2H), 4.00 (br, 4H), 3.54−3.51 (br, 8H), 2.58−2.36 (m, 12H), 1.96−1.25 (m, 24H), 0.83 (br, 3H). Anal. Calcd (%) for $(C_{44}H_{65}O_6N_3)_n$: C, 72.23, H, 8.89; N, 5.75. Found: C, 71.05; H, 8.71; N, 5.28.

Poly[(*N*-(6′-diethylphosphoryl)hexyl-2,7-carbazole)-*alt*-(2-hexyloxy-5-(6′-diethylphosphoryl)hexyloxy-1,4-phenylene)] (PCP-EP). Diethyl 6-(2,7-bis(4,4,5,5-tetramethyl-1,3,2-dioxaborolan-2-yl)carbazol-9-yl)hexylphosphonate, **3** (0.320 g, 0.5 mmol), 1,4-dibromo-2-(6-(diethylphosphoryl)hexyloxy)-5-hexyloxybenzene, **6** (0.286 g, 0.5 mmol), $Pd(PPh_3)_4$ (12 mg), and several drops of Aliquat336 were dissolved in a mixture of 12 mL of toluene and 2 mL of 2 M K_2CO_3 aqueous solution. The mixture was refluxed with vigorous stirring for 3 days under an argon atmosphere. After the mixture was cooled to room temperature, it was poured into 250 mL of hexane. The precipitated material was redissolved and filtrated through a funnel and then precipitated again. The resulting solid material was washed successively with hexane for 24 h and dried in vacuum to afford the title polymer as a white solid (351 mg, 58%). GPC: M_n = 9.3 kDa; M_w/M_n = 2.0. ^{1}H NMR ($CDCl_3$, 300 MHz), δ (ppm): 8.17 (br, 2H), 7.74 (br, 2H), 7.51 (br, 2H), 7.23 (m, 2H), 4.38 (br, 2H), 4.04(m, 12H), 1.96−1.26 (m, 40H), 0.83 (br, 3H). Anal. Calcd (%) for $(C_{44}H_{65}O_8P_2N)_n$: 66.25; H, 8.16; N, 1.76. Found: C, 64.96; H, 8.15; N, 1.51.

PLED Fabrication and Characterization. Patterned indium tin oxide (ITO)-coated glass with a sheet resistance of 15−20 ohm/square were cleaned by a surfactant scrub and then underwent a wet-cleaning process inside an ultrasonic bath, beginning with deionized water, followed by acetone and isopropanol. After oxygen plasma cleaning for 5 min, a 40 nm thick poly(3,4-ethylenedioxythiophene):poly(styrenesulfonate) (PEDOT:PSS) (Bayer Baytron 4083) anode buffer layer was spin-cast onto the ITO substrate and then dried by baking in a vacuum oven at 80 °C for overnight. For PLEDs with fluorescent PFO-DBT15 as the emissive layer, PFO-DBT15 film with a thickness of 70 nm was spin-casted from its chlorobenzene solution. For the phosphorescence devices, 1 wt % of $Ir(mppy)_3$ and 30 wt % of PBD were doped into a PVK host in chlorobenzene solution, and 70 nm thick films were formed via spin-coating. A solution of PCP-NOH or PCP-EP in methanol or methanol/water mixture was spin-coated on the top of the obtained emissive layer to form a thin interlayer of 15 nm. The

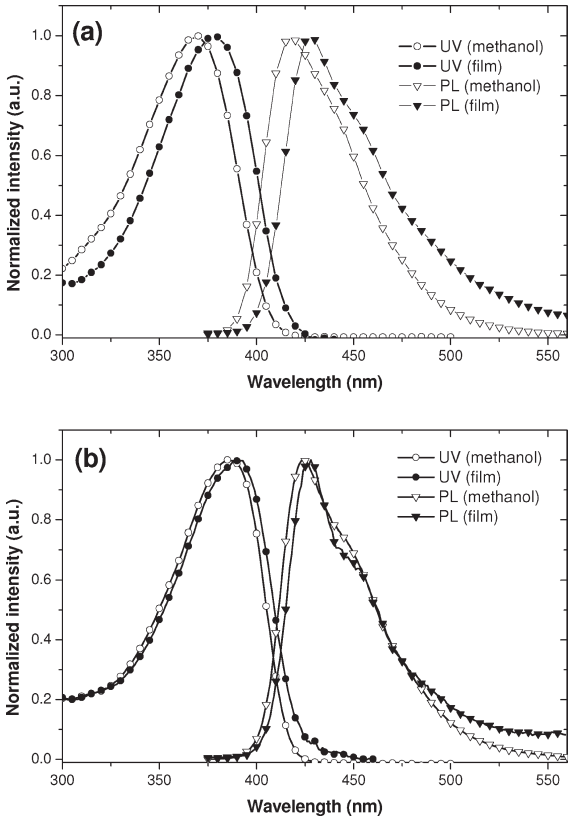

Figure 1. Normalized UV−vis absorption spectra and PL spectra of (a) PCP-NOH and (b) PCP-EP in methanol solutions and in their film states.

thickness of the PEDOT:PSS and the emissive layers were verified by a surface profilometer (Tencor, Alpha-500). Determination of the thickness of the interlayer followed a previously published paper.[13] Finally, a 100 nm aluminum layer was thermally evaporated with a shadow mask at a base pressure of 3×10^{-4} Pa. The overlapping area between the cathode and anode defined a pixel size of 0.15 cm^2. The thickness of the evaporated cathodes was monitored by a quartz crystal thickness/ratio monitor (Model: STM-100/MF, Sycon). Except for the deposition of the PEDOT:PSS layers, all the fabrication processes were carried out inside a controlled atmosphere of nitrogen drybox (Vacuum Atmosphere Co.) containing less than 10 ppm oxygen and moisture. The current−luminance−voltage (I−L−V) characteristics were recorded with a Keithley 236 source meter and a calibrated silicon photodiode. Luminance was calibrated by using a PR-705 SpectraScan spectrophotometer, and the forward-viewing LE was calculated accordingly. The external quantum efficiency was verified by measurement in the integrating sphere (IS-080, Labsphere). The electroluminescent spectra were collected by a PR-705 photometer. For photocurrent versus voltage characteristics measurements, the I−V characteristics under illumination were measured with a Keithley 236 source meter. The photocurrent was measured under solar simulator with AM 1.5G illumination (100 mW/cm^2).

RESULTS AND DISCUSSION

Synthesis of Monomers and Polymers. The synthetic routes for monomers are shown in Scheme 1. In the presence of excessive amount of 1,6-dibromohexane, the 2,7-dibromocarbazole could be transformed to a carbazole derivative **1** with a *N*-(6′-bromohexyl) group in a 72% yield. The diboronic ester compound **2** with a total yield of 83% after recrystallization in THF/ethanol mixture was synthesized by Miyaura coupling of **1** and bis(pinacolato)diboron with $PdCl_2$(dppf) as the catalyst.[38] A heating reaction of **1** in triethyl phosphate at 140 °C readily afforded a carbazole derivative **3** with phosphonate end group in a high yield of 89.1%. The synthesis of **4** was achieved in a good yield of 70% by the condensation of 4-hexyloxyphenol with 1,6-dibromohexane in a basic medium. The 1,4-dibromo compound **5** was synthesized by the bromination of **4** with bromine in CCl_4, with a good yield of 83%. A similar phosphonate transformation of **5** under heating afforded the target benzene derivative **6** in a high yield of 93%. The chemical structures of compounds **1**−**6** were confirmed by ^{1}H NMR, ^{13}C NMR, and elemental analysis (see the Experimental Section for details).

Scheme 1 also shows the polymerization routes for the two target polymers. The preparations of the PCP-EP and the intermediate polymer PCP-Br were accomplished via Pd-$(PPh_3)_4$-catalyzed Suzuki reaction of the corresponding monomers. The transformation from PCP-Br to the target polymer PCP-NOH was achieved by post-treatment of PCP-Br with diethanolamine in a mixture DMF/THF.[18] Some variations of characteristic ^{1}H NMR peaks could be found. The hydrogen resonances at 3.39 and 3.29 ppm for the two end CH_2-Br groups on the carbazole and benzene units completely disappeared in the ^{1}H NMR of PCP-NOH. New resonance peaks at 3.54−3.51 ppm for CH_2-OH and 2.58−2.36 ppm for $(CH_2)_3$N appeared. Polymers PCP-NOH and PCP-EP are easily soluble in organic solvents such as tetrahydrofuran (THF), toluene, chloroform, and dimethylformamide (DMF). Moreover, the polar diethanolamine and phosphonate groups on the side chains supply the two polymers with solubilities in methanol or ethanol to a level of over 5 mg/mL. The alcohol solutions did not become turbid if a proper proportion of water was added. Measured by GPC with calibration of polystyrene standards and THF as the eluent, the number-averaged molecular weights (M_n) of PCP-EP and the intermediate polymer PCP-Br are comparable of 9300 and 10 500, respectively, with polydispersity index (M_w/M_n) of 2.0 and 2.3, respectively. The molecular weight of PCP-NOH, a transformed product, should be comparable to that of its precursor PCP-Br, based on the high transformation yield of 82%. The chemical structures of PCP-Br, PCP-NOH, and PCP-EP were confirmed by ^{1}H NMR and elemental analysis (see the Experimental Section for details).

UV Absorption and Photoluminescence. The UV−vis absorption spectra of PCP-NOH and PCP-EP in methanol solutions and in their film states are shown in Figure 1. The PCP-NOH solution shows absorption maximum (λ_{abs}) at 369 nm (Table 1), pratically identical to λ_{abs} = 367 nm of a copolymer PCMEHP derived from 2,7-carbazole and 2,5-dialkoxy-1,4-phenylene in solution.[39] The result demonstrates that the diethanolamino groups on the side chain of PCP-NOH has very limited influence on the solution absorption of the polymer main chain. The λ_{abs} for the thin solid film of PCP-NOH slightly red-shifts to 378 nm. Compared with λ_{abs} = 368 nm for the film of PCMEHP, the calculated 10 nm red-shift of PCP-NOH indicates that the polar diethanolamino groups would have some effect on the absorption spectrum in the aggregation state. The absorption edges for the absorption spectra of the solution and the film of PCP-NOH are at 420 and 426 nm, respectively. The λ_{abs} values for the solution and the film of PCP-EP move to 385 and 389 nm, respectively, but showing a smaller aggregation effect on the absorption changing. The absorption edges for the absorption

Table 1. Optical Properties and Energy Levels of PCP-NOH and PCP-EP

	λ_{abs}[a] (nm)		λ_{em}[b] (nm)					
polymer	solution	film	solution	film	E_g[c] (eV)	E_{ox}[d] (V)	HOMO[e] (eV)	LUMO[f] (eV)
PCP-NOH	369	378	417	427	2.91	0.53	−5.21	−2.30
PCP-EP	385	389	424	428	2.83	0.52	−5.20	−2.37

[a] Absorption peak. [b] Emission peak. [c] Optical band gap. [d] Onset voltage of oxidation process during cyclic voltammetry with Ag/Ag^+ reference electrode. [e] Calculated according to HOMO = $-e(E_{ox} + 4.68)$. [f] Calculated from HOMO level and the optical band gap.

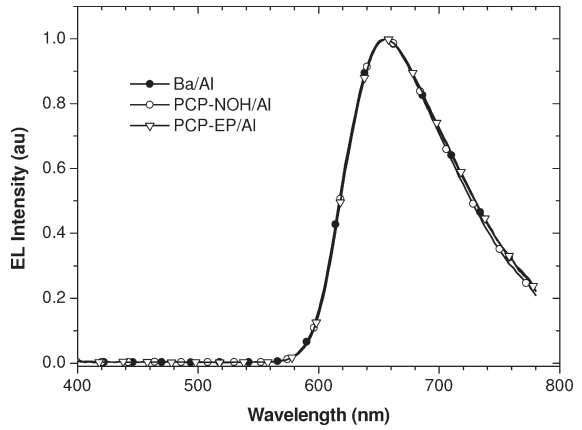

Figure 2. EL spectra of PLEDs with fluorescent PFO-DBT15 as the emissive layer by using different cathodes.

spectra of the solution and the film of PCP-EP are at 425 and 438 nm, respectively. Approximately, the phosphonate pendants on PCP-EP exhibit some contribution to enhance the conjugation length of the 2,7-carbazole-1,4-phenylene backbone, possibly due to the side-chain-induced conformational effect.

The PL spectra of PCP-NOH and PCP-EP in methanol solutions and in their film states are also shown in Figure 1. The solution and film of PCP-NOH show emission maximum (λ_{em}) at 417 and 427 nm, respectively (Table 1), comparable to the corresponding 414 and 425 nm for PCMEHP solution and film.[39] The λ_{em} values of the solution and film of PCP-EP are at 424 and 428 nm, respectively. The results illustrate that the polar diethanolamino and phosphonate groups almost do not affect the PL emissions from the polymer backbone.

Energy Level. The optical band gaps of the films of PCP-NOH and PCP-EP estimated with the absorption edges of the thin solid films are also listed in Table 1. The optical band gaps of PCP-NOH and PCP-EP are 2.91 and 2.83 eV, respectively. The HOMO levels of the polymers were obtained from the onsets of oxidation potentials (E_{ox}) during cyclic voltammetry (CV) measurements with an Ag/Ag^+ electrode as the reference electrode and an energy level of ferrocene of −4.80 eV as the internal standard. The calibrated energy level of the Ag/Ag^+ electrode is −4.68 eV. The HOMO levels of PCP-NOH and PCP-EP are arround −5.2 eV, according to their practically identical E_{ox} values of 0.52 V against the Ag/Ag^+ reference electrode. The comparable oxidation processes of PCP-NOH and PCP-EP demonstrate very limited influences of their pendants on the oxidation of the polymer backbone. The LUMO levels of the polymers were calculated from the HOMO levels and resulting optical band gaps. Thus, the deduced LUMO levels of PCP-NOH and PCP-EP of −2.30 and −2.37 eV, respectively, were obtained.

As Electron Injection Layer (EIL) in Polymer Light-Emitting Diodes. The polar and surfactant-like end groups on the side chains of PCP-NOH and PCP-EP would have strong interactions with metals, from which good electron injections from high work function metal cathodes could be expected. The special soluble properties of PCP-NOH and PCP-EP in environmental-friendly solvents such as alcohols or alcohol/water mixtures could prevent interfacial mixing between the emissive polymer layer and the conjoint EIL, during multilayer fabrications by solution processing.[11]

Multilayer PLEDs with a configuration of ITO/PEDOT:PSS (40 nm)/PFO-DBT15 (70 nm)/EIL (15 nm)/Al (100 nm) were fabricated. PFO-DBT15, a typical fluorescent polymer with saturated red-light emisson, was selected to construct the emissive layer. Then PCP-NOH and PCP-EP solutions with a concentration of 2 mg/mL in methanol were spin-casted on top of the PFO-DBT15 layer as the thin EIL. Finally, a 100 nm thickness of Al was evaporated to form the metal cathode. For a comparion study, PLEDs based on sole Al cathode without the EIL and a well-known Ba/Al cathode with a low work function metal were also fabricated so as to reveal the EIL features of PCP-NOH and PCP-EP.

The PFO-DBT15-based PLEDs with PCP-NOH and PCP-EP as the EIL emitted saturated red light with practically identical electroluminescence (EL) spectra (λ_{em} = 656 nm) to that of the Ba/Al cathode (Figure 2), demonstrating that inserting the EIL does not change the EL spectrum of the PFO-DBT15.[36] The PLED with Al cathode showed a relatively high turn-on voltage (V_{on}) of 5.9 V, and the V_{on} values of other devices were below 4 V (Table 2). Performances of the PLEDs at a comparable current density of ~39 mA/cm^2 are also listed in Table 2. The PLED with Al cathode only emitted a light with a luminance of 6 cd/cm^2 at a current density of 40.4 mA/cm^2, corresponding to an external quantum efficiency (EQE) of 0.03% and a LE of 0.015 cd/A. The PLED with low work function barium significantly improved the performance because of the enhancement of electron injection. The device displayed a practical luminance of 202 cd/cm^2, EQE of 1.16%, and LE of 0.58 cd/A, at a current density of 37.5 mA/cm^2. The PCP-NOH/Al and PCP-EP/Al bilayer cathodes could further increase the efficiency. The device with PCP-NOH/Al bilayer cathode showed EQE of 2.02% and LE of 1.01 cd/A for a luminance of 405 cd/cm^2 at a current density of 40.1 mA/cm^2, while EQE of 1.76% and LE of 0.88 cd/A for a luminance of 307 cd/cm^2 at a current density of 38.7 mA/cm^2 were realized with the PCP-EP bilayer cathode. The efficiency data realized by PCP-NOH/Al and PCP-EP/Al are higher than that of PFO-DBT15 in the literature.[36] During the increasing of current density up to 100 mA/cm^2, the PLEDs with the PCP-NOH/Al and PCP-EP/Al bilayer cathodes all showed higher efficiency in comparison to the case of Ba/Al cathode (Figure 3). The results demonstrate that both the PCP-NOH/Al and PCP-EP/Al

Table 2. Device Performances of PLEDs with Fluorescent PFO-DBT15 as the Emissive Layer by Using Different Cathodes

cathode	V_{on}[a] (V)	voltage[b] (V)	current density[b] (mA/cm^2)	luminance[b] (cd/m^2)	EQE[b] (%)	LE[b] (cd/A)
Al	5.9	7.8	40.4	6	0.03	0.015
Ba/Al	2.6	3.4	37.5	202	1.16	0.58
PCP-NOH/Al	3.8	5.2	40.1	405	2.02	1.01
PCP-EP/Al	2.7	4.5	38.7	307	1.76	0.88

[a] Turn-on voltage defined for a brightness of 1 cd/m^2. [b] Device performance at a current density of ~39 mA/cm^2.

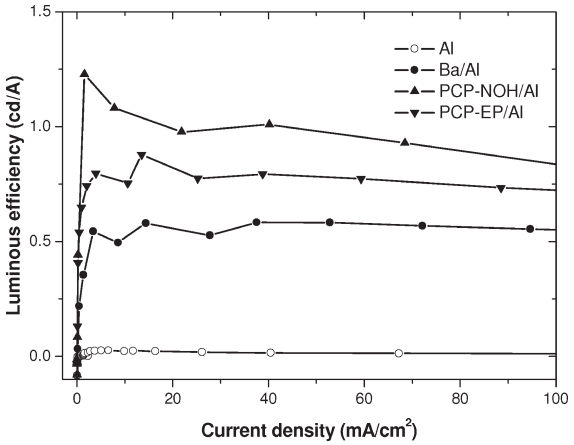

Figure 3. Luminous efficiency−current density characteristics of PLEDs with fluorescent PFO-DBT15 as the emissive layer by using different cathodes.

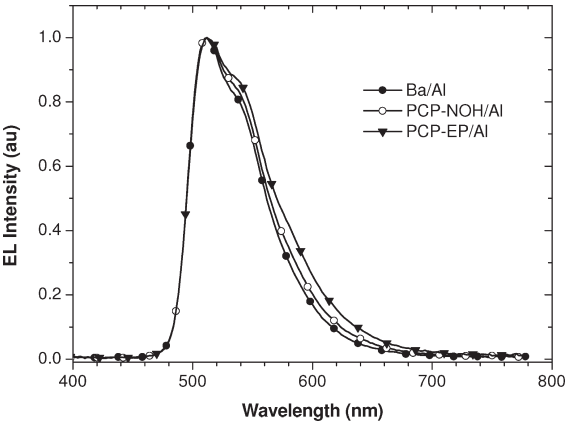

Figure 5. EL spectra of PLEDs with a phosphorescent dye-doped polymer blend (PVK:PBD:Ir(mppy)$_3$ = 100:30:1) as the emissive layer by using different cathodes.

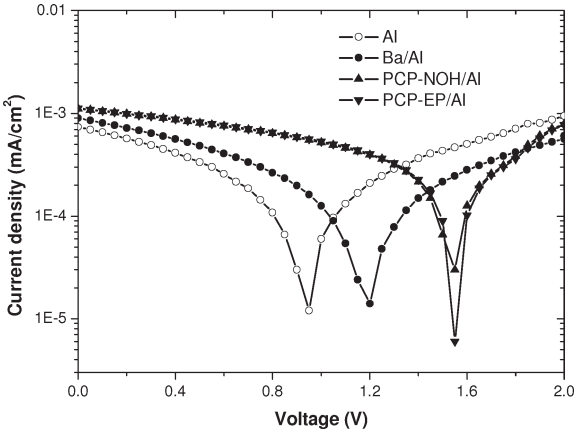

Figure 4. Photovoltaic characteristics of PFO-DBT15-based PLEDs under white light illumination with different cathodes.

bilayer cathodes can establish effective electron injections to the emissive layer.

It was reported before that the decreased electron injection barrier from the bilayer cathode to the emissive layer could be ascribed to the formation of positive interfacial dipole between the EIL and the Al electrode.[13] The polar diethanolamino and phosphonate groups should generate strong interactions with the high work function Al electrode. Open-circuit voltage, an important parameter relevant to the built-in potential across the junction and the electrodes, would reflect the interfacial characteristics of the different cathodes.[13] Figure 4 shows the photovoltaic behaviors of the PLEDs with the different cathodes. The device with Al cathode showed an open-circuit voltage (V_{oc}) of 0.95 V. The V_{oc} values increased to 1.5 V for PLEDs with PCP-NOH/Al and PCP-EP/Al bilayer cathodes, which is even higher than V_{oc} = 1.2 V for Ba/Al device. The results indicate that inserting polar interfacial layer between Al electrode and the PFO-DBT15 emissive layer can decrease the barrier height for electron injection. Thereby, the PLEDs with PCP-NOH/Al and PCP-EP/Al bilayer cathodes could significantly improve the device performances.

Electrophosphorescent light-emitting diodes have been attracting much attention because of their high device efficiency.[40,41] Electrophosphorescence can make full use of both singlet and triplet excitons owing to strong spin−orbital coupling of heavy-metal ions in phosphorescent dyes. As a result, electrophosphorescence can theoretically approach 100% internal quantum efficiency.[42] To examine the general applicability of PCP-NOH and PCP-EP for electron injection, we fabricated electrophosphorescent PLEDs with green-emitting Ir(mppy)$_3$ as the phosphorescent dye, doped in PVK host, whose device configuration was ITO/PEDOT:PSS (40 nm)/emissive layer (70 nm)/EIL (15 nm)/Al (100 nm). PBD was selected to enhance electron transport in the emissive layer. A blend ratio of PVK:PBD:Ir(mppy)$_3$ = 100:30:1 was utilized to construct the emissive layer. PCP-NOH and PCP-EP films were spin-casted from water/methanol (1:3 by volume) mixtures onto the emissive layer so as to suppress the erotion of PBD by pure methanol.[21] For comparison, PLEDs with sole Al and Ba/Al cathodes were also fabricated.

The electrophosphorescent PLED with Al cathode showed very poor device perforamance, whereas the other three PLEDs could emit highly efficient green light with same λ_{em} at 510 nm (Figure 5), ascribed to the green emission of Ir(mppy)$_3$.[37] Slight

Table 3. Device Performances of PLEDs with a Phosphorescent Dye-Doped Polymer Blend (PVK:PBD:Ir(mppy)$_3$ = 100:30:1) as the Emissive Layer by Using Different Cathodes

cathode	V_{on}[a] (V)	voltage[b] (V)	current density[b] (mA/cm^2)	luminance[b] (cd/m^2)	EQE[b] (%)	LE[b] (cd/A)	LE_{max}[d] (cd/A)	L_{max}[e] (cd/m^2)
Al	12.0	10.5	2.61	[c]			0.35	440
Ba/Al	4.0	7.5	2.27	732	9.6	32.2	32.2	26 300
PCP-NOH/Al	5.7	9.6	2.50	982	11.7	39.3	39.3	28 300
PCP-EP/Al	5.4	10.2	2.68	1078	12.0	40.1	42.5	28 500

[a] Turn-on voltage defined for a brightness of 1 cd/m^2. [b] Device performance at a current density of ~2.5 mA/cm^2. [c] No light. [d] Maximum luminous efficiency. [e] Maximum luminance.

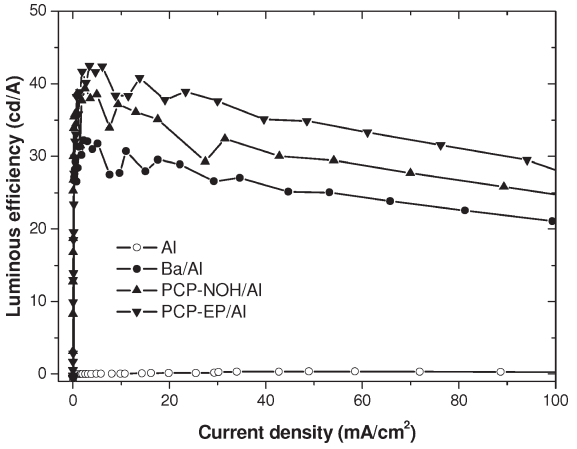

Figure 6. Luminous efficiency−current density characteristics of PLEDs with a phosphorescent dye-doped polymer blend (PVK:PBD:Ir(mppy)$_3$ = 100:30:1) as the emissive layer by using different cathodes.

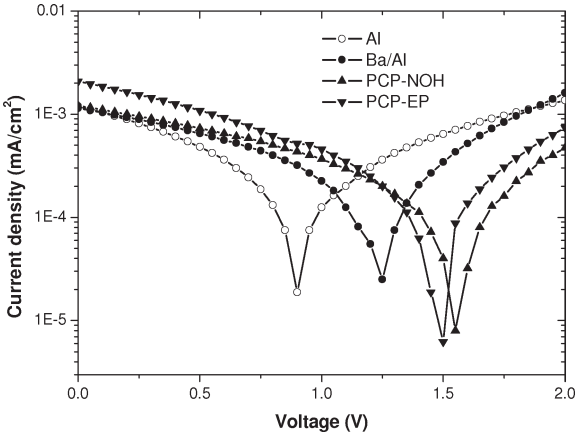

Figure 7. Photovoltaic characteristics of the electrophosphorescent PLEDs under white light illumination with different cathodes.

deviations of the EL spectra, at wavelength range between 530 and 680 nm, might be ascribed to microcavity effect when inserting the EIL. The device performances of the electrophosphorescent PLEDs at a current density of ~2.5 mA/cm^2 are summarized in Table 3. No light could be detected for the PLED with Al cathode even at a current density of 2.61 mA/cm^2, indicating a hole-only current. Using Ba/Al cathode could boost the device luminance to 732 cd/cm^2 at a current density of 2.27 mA/cm^2, corresponding to EQE of 9.6% and LE of 32.2 cd/A. The PLEDs with PCP-NOH/Al and PCP-EP/Al bilayer cathodes displayed higher efficiency than the case of the Ba/Al cathode again. The device with PCP-NOH/Al bilayer cathode showed EQE of 11.7% and LE of 39.3 cd/A for a luminance of 982 cd/cm^2 at a current density of 2.5 mA/cm^2 while EQE of 12.0% and LE of 40.1 cd/A for a luminance of 1078 cd/cm^2 at a current density of 2.68 mA/cm^2 were found for the PCP-EP bilayer cathode. The PLED with the PCP-EP bilayer cathode exhibited a maximum LE (LE_{max}) of 42.5 cd/A at a higher luminance of 1450 cd/cm^2. The LE_{max} values of the two PLEDs with the PCP-NOH/Al and PCP-EP/Al bilayer cathodes are over 100 times better than that with the sole Al cathode. The maximum luminances (L_{max}) of the two PLEDs with the PCP-NOH/Al and PCP-EP/Al bilayer cathodes are all over 28 000 cd/m^2, which are much better than the L_{max} = 440 cd/m^2 for the Al cathode and also better than the L_{max} = 26 300 cd/m^2 for the Ba/Al cathode. Except the PLED with Al cathode, the other three high-performance PLEDs showed similarly weak roll-off of efficiency at higher current density (Figure 6). Particularly, the PLED with the PCP-EP bilayer cathode still possessed an excellent LE of 33.3 cd/A at a current density of 61.1 mA/cm^2, corresponding to a much high luminance of 20 300 cd/cm^2. The results clearly demonstrate that PCP-NOH and PCP-EP are excellent electron injection polymers for high-performance PLEDs with high work function Al electrode. It should be noted that the efficiency realized with the PCP-NOH/Al and PCP-EP/Al bilayer cathodes are also significantly higher than those of Ir(mppy)$_3$-based electrophosphorescent devices (with a similar composition in the emissive layer) with Ca/Al and CsF/Al cathodes in the literature.[37]

Photovoltaic characteristics of the electrophosphorescent PLEDs under white light illumination with different cathodes are shown in Figure 7. The V_{oc} values for PLEDs with PCP-NOH/Al and PCP-EP/Al bilayer cathodes are 1.55 and 1.50 V, respectively, all higher than V_{oc} = 1.25 V for the Ba/Al cathode as well as V_{oc} = 0.9 V for the Al cathode. The V_{oc} results support the notable electron injection abilities of PCP-NOH and PCP-EP in combination with the high work function Al electrode.

It should be pointed out that the fluorescent PFO-DBT15-based PLED with PCP-NOH as the EIL showed higher efficiency than that of PCP-EP as EIL, whereas PCP-EP displayed better device performance than PCP-NOH in the electrophosphorescent PLED. Therefore, the selection of an EIL from PCP-NOH and PCP-EP needs a consideration of the chemical structure of an emitting material.

CONCLUSIONS

In summary, alcohol-soluble 2,7-carbazole-1,4-phenylene copolymers PCP-NOH and PCP-EP, comprising surfactant-like diethanolamino and phosphonate end groups on the side chains, respectively, were synthesized and utilized as interlayer for the

modification of electron injection from high work function Al electrode in PLEDs. The UV−vis absorption, photoluminescence, and energy levels of the PCP-NOH and PCP-EP were mainly determined by the conjugated 2,7-carbazole-1,4-phenylene main chain. With fluorescent PFO-DBT15 as the emissive layer, the PLEDs using the PCP-NOH and PCP-EP as the EIL displayed LE of 1.01 and 0.88 cd/A, respectively, all obviously higher than 0.015 cd/A for sole Al cathode and 0.58 cd/A for the well-known Ba/Al cathode. With a phosphorescent $Ir(mppy)_3$-doped polymer blend (PVK:PBD:$Ir(mppy)_3$ = 100:30:1) as the emissive layer, the PLEDs with the EIL showed outstanding LE_{max} of 39.3 cd/A for PCP-NOH and 42.5 cd/A for PCP-EP, in comparison to 0.35 cd/A for sole Al cathode and 32.2 cd/A for the Ba/Al cathode. The PLEDs with the EIL also showed weak roll-off of efficiency at high current density. Inserting the polar alcohol-soluble polymers as interlayer could significantly increase built-in potentials in the PLEDs, from which electron injection barrier from the Al electrode was decreased. The results indicate that the PCP-NOH and PCP-EP are excellent electron injection polymers for high-performance PLEDs with high work function Al electrode.

AUTHOR INFORMATION

Corresponding Author

*E-mail: psjwchen@scut.edu.cn; Fax: +8620-8711-0606.

ACKNOWLEDGMENT

We gratefully acknowledge the financial support of National Natural Science Foundation of China (Nos. 50773023, 50990065, and 51010003), National Basic Research Program of China (973 program No. 2009CB623600), and SCUT Grant (No. 2009-ZZ0003).

REFERENCES

(1) Burroughes, J. H.; Bradley, D. D. C.; Brown, A. R.; Marks, R. N.; Mackay, K.; Friend, R. H.; Burn, P. L.; Holmes, A. B. *Nature* **1990**, *347*, 539.

(2) (a) Grimsdale, A. C.; Chan, K. L.; Martin, R. E.; Jokisz, P. G.; Holmes, A. B. *Chem. Rev.* **2009**, *109*, 897. (b) Wu, H. B.; Ying, L.; Yang, W.; Cao, Y. *Chem. Soc. Rev.* **2009**, *38*, 3391.

(3) *Organic Light-Emitting Devices: synthesis, properties and applications*; Mullen, K., Scherf, U., Eds.; Wiley-VCH: Weinheim, 2006.

(4) Lee, Y. Z.; Chen, X.; Chen, S. A.; Wei, P. K.; Fann, W. S. *J. Am. Chem. Soc.* **2001**, *123*, 2296.

(5) Hung, L. S.; Tang, C. W.; Mason, M. G. *Appl. Phys. Lett.* **1997**, *70*, 152.

(6) Piromerium, P.; Oh, H.; Shen, Y.; Malliaras, G. G.; Scott, J. C.; Brock, P. J. *Appl. Phys. Lett.* **2000**, *77*, 2403.

(7) Cao, Y.; Yu, G.; Heeger, A. J. *Adv. Mater.* **1998**, *10*, 917.

(8) Yang, X.; Mo, Y.; Yang, W.; Yu, G.; Cao, Y. *Appl. Phys. Lett.* **2001**, *79*, 563.

(9) Hoven, C. V.; Garcia, A.; Bazan, G. C.; Nguyen, T. Q. *Adv. Mater.* **2008**, *20*, 3793.

(10) Jiang, H.; Taranekar, P.; Reynolds, J. R.; Schanze, K. S. *Angew. Chem., Int. Ed.* **2009**, *48*, 4300.

(11) Huang, F.; Wu, H. B.; Cao, Y. *Chem. Soc. Rev.* **2010**, *39*, 2500.

(12) Huang, F.; Wu, H.; Wang, D. L.; Yang, W.; Cao, Y. *Chem. Mater.* **2004**, *16*, 708.

(13) Wu, H.; Huang, F.; Mo, Y.; Yang, W.; Wang, D.; Peng, J.; Cao, Y. *Adv. Mater.* **2004**, *16*, 1826.

(14) Huang, F.; Hou, L. T.; Wu, H. B.; Wang, X. H.; Shen, H. L.; Cao, W.; Yang, W.; Cao, Y. *J. Am. Chem. Soc.* **2004**, *126*, 9845.

(15) Ma, W.; Iyer, P. K.; Gong, X.; Liu, B.; Moses, D.; Bazan, G. C.; Heeger, A. J. *Adv. Mater.* **2005**, *17*, 274.

(16) Wu, H. B.; Huang, F.; Peng, J. B.; Cao, Y. *Org. Electron.* **2005**, *6*, 118.

(17) Zeng, W. J.; Wu, H. B.; Zhang, C.; Huang, F.; Peng, J. B.; Yang, W.; Cao, Y. *Adv. Mater.* **2007**, *19*, 810.

(18) Huang, F.; Niu, Y. H.; Zhang, Y.; Ka, J. W.; Liu, M. S.; Jen, A. K. Y. *Adv. Mater.* **2007**, *19*, 2010.

(19) Zhang, Y.; Huang, F.; Chi., Y.; Jen, A. K. Y. *Adv. Mater.* **2008**, *20*, 1565.

(20) Huang, F.; Shih, P. I.; Shu, C. F.; Chi, Y.; Jen, A. K. Y. *Adv. Mater.* **2009**, *21*, 361.

(21) Huang, F.; Zhang, Y.; Liu, M. S.; Jen, A. K. Y. *Adv. Funct. Mater.* **2009**, *19*, 2457.

(22) Guo, X.; Qin, C. J.; Cheng, Y. X.; Xie, Z. Y.; Geng, Y. H.; Jing, X. B.; Wang, F. S.; Wang, L. X. *Adv. Mater.* **2009**, *21*, 3682.

(23) Yang, R. Q.; Wu, H. B.; Cao, Y.; Bazan, G. C. *J. Am. Chem. Soc.* **2006**, *128*, 14422.

(24) Yang, R. Q.; Garcia, A.; Korystov, D.; Mikhailovsky, A.; Bazan, G. C.; Nguyen, T. Q. *J. Am. Chem. Soc.* **2006**, *128*, 16532.

(25) Zhang, L.; He, C.; Chen, J.; Yuan, P.; Huang, L.; Zhang, C.; Cai, W.; Liu, Z.; Cao, Y. *Macromolecules* **2010**, *43*, 9771.

(26) Luo, J.; Wu, H. B.; He, C.; Li, A. Y.; Yang, W.; Cao, Y. *Appl. Phys. Lett.* **2009**, *95*, 043301.

(27) Na, S. I.; Oh, S. H.; Kim, S. S.; Kim, D. Y. *Org. Electron.* **2009**, *10*, 496.

(28) Seo, J. W.; Gutacker, A.; Walker, B.; Cho, S.; Garcia, A.; Yang, R.; Nguyen, T. Q.; Heeger, A. J.; Bazan, G. C. *J. Am. Chem. Soc.* **2009**, *131*, 18220.

(29) Lan, L.; Peng, J.; Sun, M.; Zhou, J.; Zou, J.; Wang, J.; Cao, Y. *Org. Electron.* **2009**, *10*, 346.

(30) Blouin, N.; Leclerc, M. *Acc. Chem. Res.* **2008**, *41*, 1110.

(31) Boudreault, P. L. T.; Morin, J. F.; Leclerc, M. In *Design and Synthesis of Conjugated Polymer*; Leclerc, M., Morin, J. F., Eds.; Wiley-VCH: Weinheim, Germany, 2010; pp 205−226.

(32) Bellows, D.; Gingras, E.; Aly, S. M.; Abd-El-Aziz, A. S.; Leclerc, M.; Harvey, P. D. *Inorg. Chem.* **2008**, *47*, 11720.

(33) Fruth, A.; Klapper, M.; Mullen, K. *Macromolecules* **2010**, *43*, 467.

(34) Zhang, M.; Fan, H.; Guo, X.; He, Y.; Zhang, Z.; Min, J.; Zhang, J.; Zhao, G.; Zhan, X.; Li, Y. *Macromolecules* **2010**, *43*, 5706.

(35) Zhou, E.; Cong, J.; Yamakawa, S.; Wei, Q.; Nakamura, M.; Tajima, K.; Yang, C.; Hashimoto, K. *Macromolecules* **2010**, *43*, 2873.

(36) Hou, Q.; Xu, Y.; Yang, W.; Yuan, M.; Peng, J.; Cao, Y. *J. Mater. Chem.* **2002**, *12*, 2887.

(37) Yang, X.; Neher, D.; Hertel, D.; Daubler, T. K. *Adv. Mater.* **2004**, *16*, 161.

(38) Ishiyama, T.; Murata, M.; Miyaura, N. *J. Org. Chem.* **1995**, *60*, 7508.

(39) Morin, J. F.; Boudreault, P. L.; Leclerc, M. *Macromol. Rapid Commun.* **2002**, *23*, 1032.

(40) Baldo, M. A.; O'Brien, D. F.; You, Y.; Shoustikov, A.; Sibley, S.; Thompson, M. E.; Forrest, S. R. *Nature* **1998**, *395*, 151.

(41) Chen, X. W.; Liao, J. L.; Liang, Y.; Ahmed, M. O.; Tseng, H.-E.; Chen, S. A. *J. Am. Chem. Soc.* **2003**, *125*, 636.

(42) Liu, J.; Pei, Q. B. *Macromolecules* **2010**, *43*, 9608.